CHEMISTRY
A EUROPEAN JOURNAL

DOI: 10.1002/chem.200601492

Tryptophan-Based Peptides to Synthesize Gold and Silver Nanoparticles: A Mechanistic and Kinetic Study

Satyabrata Si and Tarun K. Mandal*[a]

Abstract: Synthetic oligopeptides with a tryptophan residue at the C-terminus have been used for the synthesis of gold and silver nanoparticles at pH 11. The tryptophan residue in the peptides is responsible for the reduction of metal ions to the respective metals, possibly through electron transfer. A mechanistic pathway has been proposed to explain the reductive properties of the tryptophan moiety of the peptide based on some spectroscopic techniques, such as UV-visible and fluorescence spectroscopy. This study reveals that some of the peptide molecules are converted to its corresponding ditryptophan, kynurenine form and some cross-linked products, all of which are highly fluorescent species. The resultant peptide-functionalized metal nanoparticles have also been characterized by UV-visible spectroscopy, transmission electron microscopy, and Fourier transform IR spectroscopy and thermogravimatric analysis.

Keywords: gold nanoparticles · kinetics · reaction mechanisms · peptides · silver nanoparticles · tryptophan

Introduction

Synthesis of metal nanoparticles (MNPs) of various size and shape and their colloidal stabilization through biomolecule immobilization is very essential due to their usefulness in many biotechnological applications, such as sensors,[1–3] catalysis,[4,5] and bioanalytical processes.[6–8] Among the various MNPs, gold (Au) and silver (Ag) nanoparticles are extensively studied due to their interesting optoelectronic properties.[9] In addition, these NPs can be used as an optical probes as a result of their color change upon the coupling of surface plasmon resonances of adjacent nanoparticles. They are also very convenient for use in various bioanalytical applications.[6] These colloidal MNPs are generally prepared by borohydride/citrate reduction of metal salts followed by ligand exchange with a suitable organic molecule/biomolecule containing a SH or NH_2 group as a stabilizer, and in some cases NPs have also been prepared by reducing the metal ions in the presence of a stabilizer.[4,10] One of the disadvantages of this method is that there is always a chance of particle aggregation during the process of ligand exchange and centrifugation for the removal of the undesired product.[11] Thus, it is very important to adopt the in situ reduction technique, which can minimize the above-mentioned problems. In this method, the need of an external reducing agent, such as $NaBH_4$ or sodium citrate, can be eliminated because the stabilizing molecule itself acts as a reductant. Nowadays, many researchers are using molecules with amine functionalities as in situ reductants for the synthesis of colloidal MNPs; however, this requires higher temperatures.[12,13] Thus the ambient-temperature in situ reduction technique is very important due to its compatibility with various biological systems and its ease of use.

It has been well-established that amino acids, such as tyrosine or tryptophan, can act as stable or transient intermediates in electron/hydrogen transport in biological systems through tyrosine or tryptophan radical intermediates.[14–20] The electron-transfer process in tryptophan occurs through the formation of a tryptophyl radical, which is mainly observed in some biological systems, such as cytochrome *c* peroxidase,[15,16] Y122F mutant *Escherichia coli* RNR,[17,18] and DNA photolyase.[19,20] As reported in the literature, the tryptophan radical exists in two forms, neutral or cationic, for example, depending on whether the nitrogen atom of the tryptophan has lost its proton or not.[21] Thus the utilization of these intermediates for transferring electrons to the metal ion to generate a neutral metal atom is a new and interesting approach for synthesizing MNP clusters. However, only a few pieces of work have been reported for the preparation of metal nanoparticles by using peptides containing tyrosine

[a] S. Si, Dr. T. K. Mandal
Polymer Science Unit & Centre for Advanced Materials
Indian Association for the Cultivation of Science
Jadavpur, Kolkata 700 032 (India)
Fax: (+91) 33-2473-2805
E-mail: psutkm@mahendra.iacs.res.in

Supporting information for this article is available on the WWW under http://www.chemeurj.org/ or from the author.

as a reducing agent.[22–25] Very recently, we have reported the formation of gold nanoparticles (GNPs) by using some tyrosine-based oligopeptides.[23] Following this work, we have also reported a mechanistic and kinetic study of the formation of GNPs by using these tyrosine-based oligopeptides.[26] But up till now, no work has been reported which utilizes tryptophan-based peptides to prepare MNPs, except for the work of Sastry et al., in which they have reported the preparation of GNPs by using neat tryptophan and the oxidative polymerization of the tryptophan during the reduction process.[13]

In this report, we have designed some new oligopeptides with at least a tryptophan residue at the C-terminus, and we have used these oligopeptides to prepare Au and Ag NPs from the respective metal salts in alkaline medium. The formation mechanism of these MNPs by using the redox-active tryptophan residue of these synthetic peptides and the oxidative transformation of the respective tryptophan moiety were investigated by using various spectroscopic techniques.

Results and Discussion

It has been reported that amino acids such as tyrosine have strong electron-donating properties, which are currently being utilized for the reduction of the Au^{III} ion to metallic Au.[22] In our earlier work, we have utilized this property of tyrosine residues of short synthetic peptides to prepare gold nanoparticles (GNPs) and we have studied in detail the mechanism of reduction of gold salts and the kinetics of GNP formation.[23,26] This study prompted us to investigate the possibility of synthesizing MNPs by using tryptophan-containing peptides. Therefore, we synthesized two new peptides, peptide-1 (NH_2-Leu-Aib-Trp-OMe) and peptide-2 (Boc-Leu-Aib-Trp-OH), which contain a tryptophan residue at the C-terminus. Peptide-1 with a free N-terminus was then used to prepare metal nanoparticles (MNPs) at pH $\approx$11. For a comparative study, another peptide with the same sequence as peptide-1, but in which the N-terminus was protected with a *tert*-butyloxycarbonyl (Boc) group was also used for MNP synthesis. To increase the solubility in the reaction medium, the C-terminus ester group (OMe) of the second peptide was hydrolyzed and was designated as peptide-2.

The formation of GNPs by using peptide-1 was indicated by the visual appearance of a ruby-red colored solution and was confirmed by UV-visible spectroscopy. Figure 1a shows the absorption spectrum of the peptide-1–GNP conjugate suspension, exhibiting a surface plasmon resonance (SPR) band at 535 nm, characteristic of colloidal GNPs within a size range of 20 nm.[27] However, the spectrum of the GNPs suspension prepared by peptide-2, which contains the protected amino group, shows the SPR band at 530 nm along with a broad band at a higher wavelength region (Figure 1b). The appearance of a higher wavelength SPR band might be due to the aggregation of less-stable peptide-2–GNPs as a result of the absence of the interacting amino

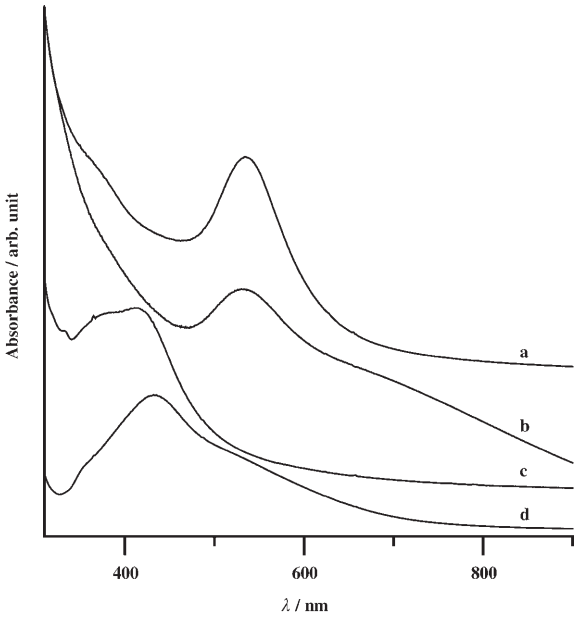

Figure 1. UV-visible absorption spectra of the GNPs suspension prepared by using a) peptide-1 and b) peptide-2 and those of the SNPs suspension prepared by using c) peptide-1 and d) peptide-2.

group with the GNPs surface. For silver nanoparticles (SNP) synthesis, peptide-1 was similarly treated with $AgNO_3$ solution. The UV-visible absorption spectrum of the resultant SNPs suspension exhibits a SPR at 415 nm along with a weaker band at $\approx$370 nm (Figure 1c). The lower wavelength SPR band is due to the formation of very small SNPs. According to the literature report, SNPs of sizes below 2 nm show a metal–nonmetal transition, and this results in the development of the lower wavelength SPR band.[28] Similarly, the UV-visible absorption spectrum of the SNPs suspension prepared with peptide-2 shows the SPR band at 432 nm along with a broad band in the higher wavelength region (Figure 1d). To check the versatility of this peptide-based method for the generation of other metal nanoparticles, these peptides were reacted with platinum and copper salts. However, we observed that the tryptophan residues of these peptides were not able to reduce Pt^{4+} and Cu^{2+}; this might be due to the huge difference in standard reduction potentials of the tryptophan residues (standard value $= 1.05 \pm 0.01$)[29] with those of the above-mentioned two metal ions.

The anchoring of the peptides (peptide-1 and -2) on the GNPs surface was confirmed through thermogravimetric analysis (TGA) of the purified peptide–GNP composites. Figure 2 shows the TGA thermograms of peptide-1–GNP and -2–GNP conjugates, which reveal the nearly similar nature of weight loss with the decomposition of peptides starting at $\approx$160 °C for both the case. This result clearly indicates that peptides are anchored on the GNPs surface.

The presence of the peptides on the GNPs surface was further confirmed from a FTIR study of the peptide–GNP conjugates. The FTIR spectrum of neat peptide-1 in Figure 3a shows the amide I and amide II bands at 1664 and

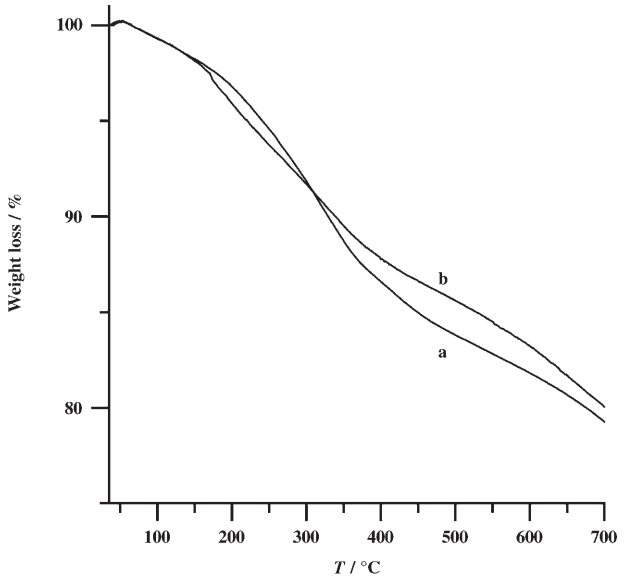

Figure 2. TGA thermograms of a) peptide-1–GNP and b) peptide-2–GNP conjugates.

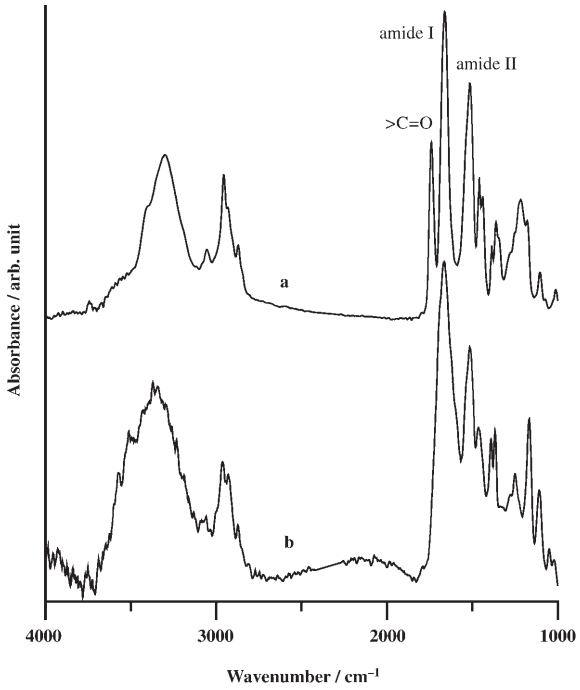

Figure 3. FTIR spectra of a) neat peptide-1 and b) peptide-1–GNP conjugates.

1512 cm^{-1}, respectively, and the ester carbonyl vibration band at 1740 cm^{-1}. Figure 3b shows the FTIR spectrum of peptide-1–GNP conjugates after removal of the excess unadsorbed peptide-1 by centrifugation and is compared with the neat peptide-1. The spectrum of peptide-1–GNPs shows two prominent bands at 1664 and at 1515 cm^{-1} corresponding to the bands produced by amides I and II of peptide-1, respectively. Thus, the presence of these bands confirms the presence of the peptides on the GNPs surface. However, the absence of the band due to the carbonyl of the ester moiety of peptide-1 indicates the hydrolysis of the ester moiety under our experimental conditions. In our earlier study, we proved that the ester (OMe) group of tyrosine containing peptides hydrolyzed to the corresponding sodium carboxylate during the reduction of gold salt to metallic gold under alkaline pH.[26] The surface attached hydrolyzed peptides might exert extra stability to the GNPs suspension. The position and nature of the amide bands in the peptide-1–GNP conjugates are same as those of the neat peptide-1, which indicates that peptide-1 does not adopt any conformational change on binding to the GNPs surface.

The transmission electron microscopic (TEM) images (Figure 4) of the peptide-based metal nanoconjugates reveal the formation of spherical particles for both gold and silver (see Supporting Information for additional TEM micrographs). The average diameters of the peptide-1–GNP and peptide-1–SNP conjugates were calculated to be 13.39 ± 2.7 and 13.66 ± 2.0 nm respectively, taking at least 50 particles into consideration. These results confirm that particles of the same size are produced in both the cases, but the size distribution of SNPs is a little bit better than that of the GNPs. TEM micrographic analysis of peptide-1–SNPs (Figure 4B) also shows some very small particles (3.18 ± 0.5 nm) in the background along with the bigger particle and this particles size corresponds well to the first SPR band observed at 370 nm for the SNPs suspension as shown in Figure 1c. Figure 4C shows the TEM micrograph of GNPs prepared with peptide-2 (see Supporting Information for additional TEM micrographs). The average diameter of the peptide-2–GNPs was calculated to be 7.33 ± 0.8 nm. By comparison, average particle size of peptide-2–GNPs is much lower and the size distribution is much narrower than that of GNPs prepared by peptide-1 containing the free amino group. This result indicated that particles of smaller size and better distribution were obtained when GNPs were prepared with peptide-2. But the colloidal stability of the formed peptide-2–GNPs suspension was less than that of the peptide-1–GNPs suspension due to the absence of free amino groups. As a result, some of the peptide-2-coated GNPs form aggregates which appear to be oblonglike in shape as seen in some parts of the TEM grid (see Figure 4C). Such oblong-shaped GNPs present in aqueous suspension might be responsible for exhibiting a low-intensity SPR band at higher wavelength (Figure 1b). In the case of peptide-2-based GNP synthesis, the formation of smaller size nanoparticles are quite contradictory to the expected result, which can be explained from the kinetic study of GNPs formation by using peptide-1 and -2.

The kinetics of the formation of GNPs at pH 11 by using peptide-1 was studied by the evaluation of their absorption spectra by taking the metal salt solution along with the peptide solution in a quartz cuvette (path length = 1.0 cm). Visually, the yellow-colored gold salt solution changed instantly to orange-red, after the addition of peptide solution. The

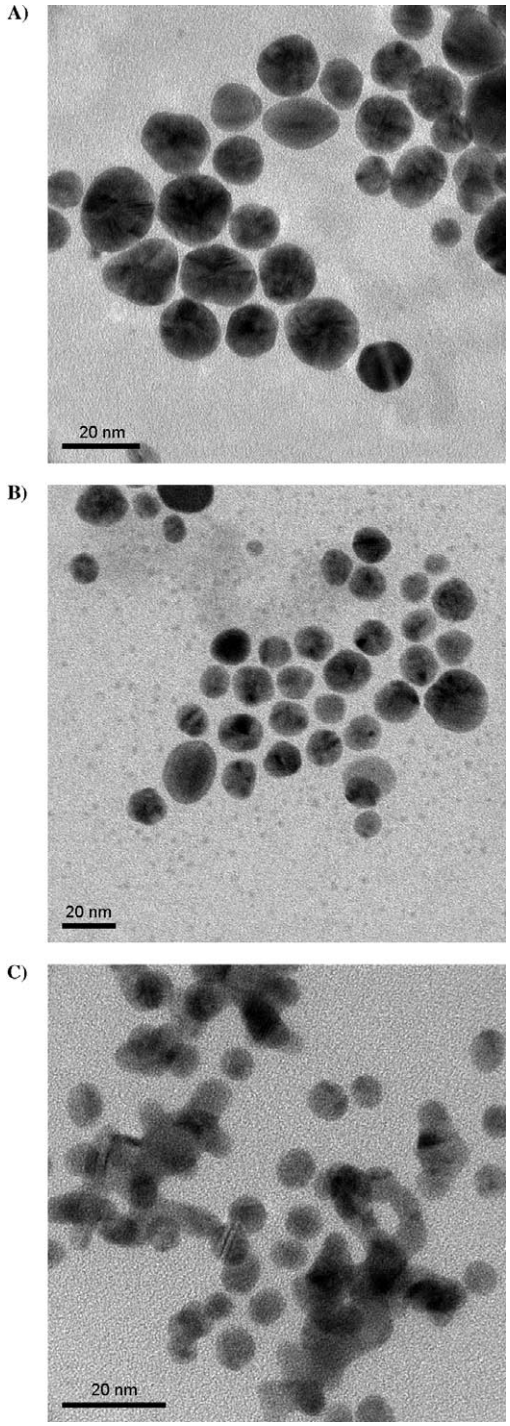

Figure 4. TEM micrographs of A) GNPs prepared with peptide-1, B) SNPs prepared with peptide-1, and C) GNPs prepared with peptide-2.

corresponding UV-visible spectrum indicates the development of a weak SPR band at $\approx$500 nm. The orange-red color subsequently faded and a decrease in the 500 nm SPR band intensity was observed in the absorption spectrum. In earlier studies, Duff et al. have also reported the formation of GNPs of subnanometer size which exhibit a weak SPR band at around 500 nm.[30] Finally, this band shifted to higher wavelength and exhibited a sharp SPR band at 535 nm due to the formation of GNPs of bigger size (10–30 nm). The plot of the change of absorbance of the SPR band at 535 nm corresponding to formed colloidal GNPs, shows a decrease in absorbance up to 8 min of reaction time, after which it increases linearly up to 50 min of reaction time (shown in arrows in Figure 5A). After that the rate becomes slower and increases linearly with time. The exact reason for the decreasing absorbance during the initial stage of the reaction is still not clear and requires further investigation. But the kinetics of the formation of GNPs by using peptide-2 shows the development of a SPR band just after the addition of peptide at pH 11, the absorbance of which subsequently goes on increasing with time. The plot of the change of absorbance of the SPR band maximum at 530 nm in Figure 5B shows a sudden increase in the absorbance within 4 min of reaction time (shown in arrow) and after that it increases slowly but linearly with time. From these two kinetics studies, it is clearly observed that the formation of GNPs with peptide-1 is much slower relative to that of peptide-2. Therefore, we can assume that in the case of peptide-1, the initially formed very small-sized GNPs (orange-red colored solution) act as seeds and results in the formation of larger particles at the latter part of the reaction. Peptide-1 contains two anchoring sites, the indole NH and the free NH_2 group. Thus, the formed particles were simultaneously anchored through the above-mentioned two functional groups, which resulted in stabilization of the larger-sized GNPs without any aggregation, thus exhibiting a sharp SPR band as shown in Figure 1a. However, in the case of peptide-2, the formed GNPs were stabilized as a result of the anchoring of only the indole NH group of the tryptophan moiety of the peptide, as there were no other groups that interact with the GNPs surface. As the indole NH groups were not sufficient to stabilize the GNPs during their formation, the TEM picture showed clusterlike aggregated particles, which resulted in the appearance of a broad SPR band in the higher wavelength region (Figure 1b).

UV-visible and fluorescence spectroscopic measurements were carried out to investigate the mechanism of reduction by the tryptophan residue of the peptides. The UV-visible spectrum (Figure 6a) of the neat peptide-1 showed a sharp absorbance peak at 280 nm, which remain unchanged in terms of peak position and its nature after the addition of the $HAuCl_4$ solution. However, the spectrum (Figure 6b) taken after three days of reaction shows that the tryptophan absorption peak broadens and blue shifts to 265 nm along with the development of a new band at $\approx$320 nm during the reduction process. This result indicates that the tryptophan moiety of the peptide is responsible for the reduction of Au^{III} ion to the neutral Au atom. Sastry et al. have also reported the synthesis of GNPs by using neat tryptophan molecules and observed the similar type of shifting of the tryptophan absorption band.[13] The development of the new band at 320 nm indicates the formation of new species that may be a modification product of the tryptophan moiety of the peptide (shown by arrow in Figure 6).

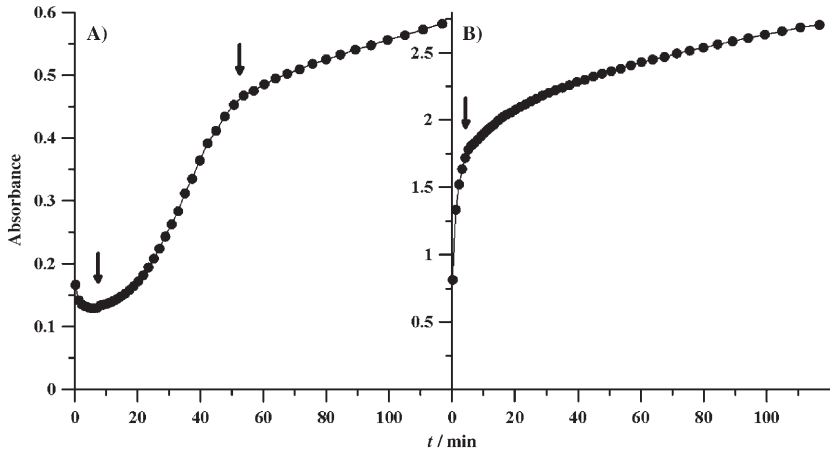

Figure 5. UV-visible kinetic study of GNP formation at pH 11 by using A) peptide-1 and B) peptide-2.

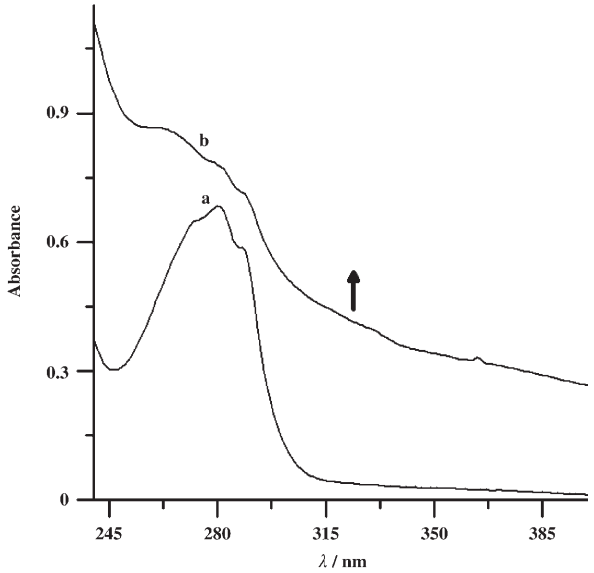

Figure 6. UV-visible absorption spectra of the tryptophan moiety in peptide-1 recorded a) at the beginning of reaction and b) after 3 d of reaction during the formation of GNPs.

We have already reported in our earlier work that the tyrosine residue of the peptide was converted to the corresponding dityrosine form during the reduction of the Au^{III} salt to neutral Au in the reaction medium.[26] Like that of tyrosine, the tryptophan residue of the peptide also has a strong electron-donating nature, which can reduce the metal salt to its corresponding neutral metal atom and itself undergo oxididation. Furthermore, it has been reported that the oxidation of tryptophan results in the formation of a number of byproducts, such as ditryptophan, kynurenine, 3-hydroxy-kynurenine, N-formyl-kynurenine, and some cross-linked products, formed by reaction with these byproducts.[31–37] Each of these byproducts has a specific absorption and shows strong emission, which provides the basis for identifying a particular species (for example, tryptophan: $E_{em}=365$, $E_{ex}=280$ nm; ditryptophan: $E_{em}=270$–280, $E_{ex}=320$ nm; N-formyl-kynurenine: $E_{em}=410$–430, $E_{ex}=310$–330 nm; kynurenine: $E_{em}=460$, $E_{ex}=365$ nm; cross-linked products: $E_{em}=520$, $E_{ex}=410$ nm). According to the literature report, the formation of these byproducts occurs only through the formation of the tryptophyl radical.[31] However, we could not detect this radical by electron paramagnetic resonance (EPR) in the reaction medium, which might be due to the poor stability of the tryptophyl radical in water. In this medium, the radical signal is either quenched by water or by the formed metal nanoparticles as reported earlier.[38–40] However, we have identified these byproducts by using fluorescence spectroscopy. Figure 7 shows the emission spectra of the neat peptide-1 solution, which shows the tryptophan

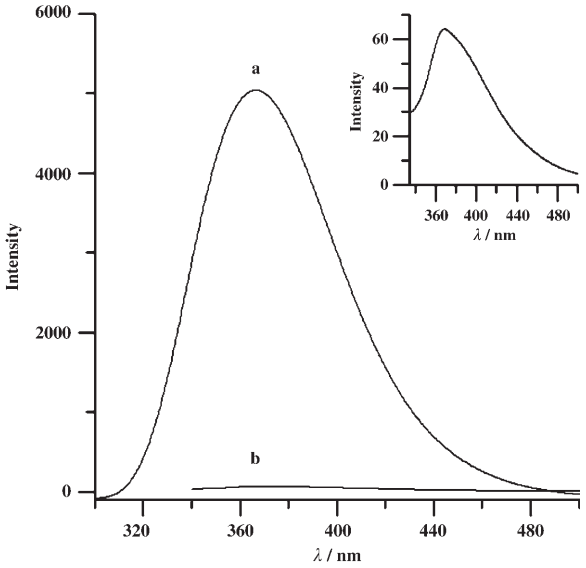

Figure 7. Emission spectra of a solution of neat peptide-1 in water. a) $E_{em}=366$, $E_{ex}=280$ nm and b) $E_{em}=366$, $E_{ex}=320$ nm (Inset shows the enlarged view of spectrum (b).

emission maximum at 366 nm when excited at 280 nm. Upon excitation at 320 nm, which is the absorption maximum of one of the oxidation products of tryptophan, the emission appears at the same position (detected from an enlarged view of the spectrum given in the inset of Figure 7) with a large decrease in intensity; this indicates the absence of any of the above-mentioned oxidation products of tryptophan in neat peptide-1.

Figure 8 shows the fluorescence spectra of peptide-1–GNPs after repeated washing to remove the excess unadsorbed peptides. The peptides when attached to the GNPs sur-

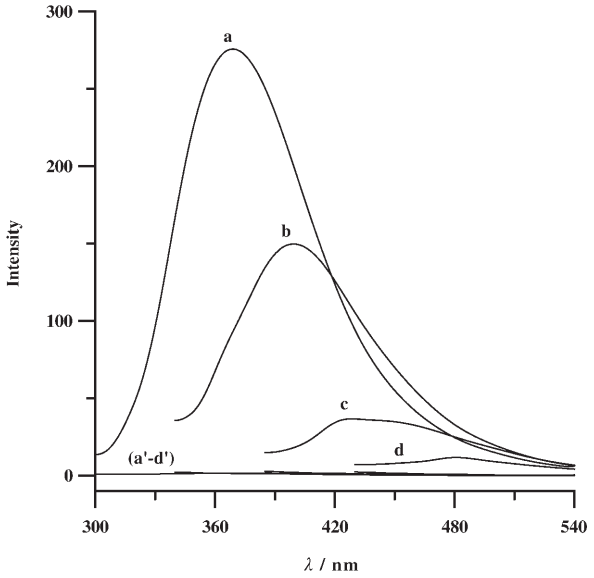

Figure 8. Emission spectra of peptide-1, desorbed from the GNPs surface by ligand exchange with MUA. a) $E_{em}=370$, $E_{ex}=280$ nm; b) $E_{em}=395$, $E_{ex}=320$ nm; c) $E_{em}=460$, $E_{ex}=365$ nm; d) $E_{em}=481$ and $E_{ex}=410$ nm. The emission spectra of adsorbed peptide-1 on the GNPs surface. a′) $E_{ex}=280$ nm; b′) $E_{ex}=320$ nm; c′) $E_{ex}=365$ nm; d′) $E_{ex}=410$ nm.

face did not show any emission corresponding to tryptophan residue/oxidation product of the tryptophan residue as a result of the fluorescence quenching by the GNPs[26,41–43](see the spectra a′–d′ in Figure 8). In order to detect the formation of any oxidation product of tryptophan, the adsorbed peptides/oxidation products on the GNPs surface were required to be exchanged with a better ligand. We chose mercaptoundecanoic acid (MUA), a better ligand, which was added in excess to the peptide-1–GNPs and stirred for 24 hours. As the interaction of the SH group in MUA with the GNPs surface is greater relative to that of the NH_2/NH group, it replaces all the peptides attached to the GNPs surface. After exchange reaction, the mixture was centrifuged to separate the MUA-capped GNPs, and the supernatant containing the surface desorbed peptides for fluorescence measurement was collected. Figure 8 shows a set of fluorescence spectra for the supernatant, at various excitation values. When excited at 280 nm, it emitted at 370 nm, whereas on excitation at 320 nm, an emission peak appeared at 395 nm. Also there was a small emission peak at 460 nm when excited at 365 nm. From Figure 8 it was also clear that the emission intensity at 370 nm was much higher compared to that of other peaks. This result indicates that most of the tryptophan moiety retains its native structure, whereas some parts dimerize to the corresponding ditryptophan (emits at 395 nm) and kynurenine (emits at 460 nm) form of the peptide, which are reported to be a highly fluorescent compounds. Besides this, some cross-linked products might also be formed, which was confirmed from the emission at 481 nm upon excitation at 410 nm.

To provide more evidence for the formation of oxidation products of tryptophan during the reduction of metal ions, GNPs were first prepared by using pepide-2, and after completion of the reaction, the attached peptide-2 and/or its oxidation product were extracted by dissolving the GNPs with KCN solution. The fluorescence spectra (Figure 9A) of the

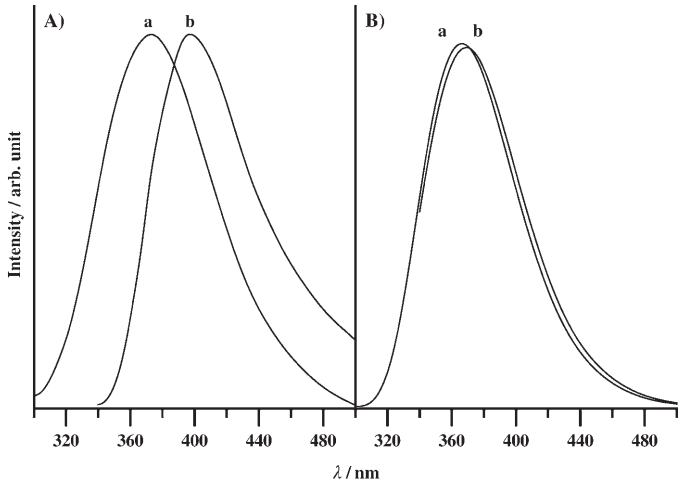

Figure 9. A) Emission spectra of peptide-2, desorbed from the GNPs surface by treatment with KCN: a) $E_{em}=370$, $E_{ex}=280$ nm and b) $E_{em}=395$, $E_{ex}=320$ nm. B) Fluorescence spectroscopic study of peptide-2 in absence of any metal salt: a) $E_{em}=370$, $E_{ex}=280$ nm and b) $E_{em}=370$, $E_{ex}=320$ nm.

resultant detached peptide-2 also shows the similar type of emission spectra as discussed earlier, for example, $E_{em}=370$, $E_{ex}=280$ nm and $E_{em}=395$, $E_{ex}=320$ nm. A control reaction was also performed to resolve the above-mentioned issue in more detail. Peptide-2 was kept stirring in absence of any metal ions for three days at pH $\approx$11 and the emission spectra of the resultant solution were recorded. Figure 9B showed that the emission peak position remained unchanged irrespective of the excitation value ($E_{em}=370$, $E_{ex}=280$ and 320 nm) for that of neat tryptophan containing peptides. This clearly indicates that the tryptophan moiety of the peptide does not convert to any of its oxidized forms in absence of metal ions.

Thus, from the above discussion we can summarize that in the presence of metal ions, the tryptophan moiety donates an electron to the nearby metal ion and thereby forms the tryptophyl radical, which is subsequently transferred to its different oxidized form as shown in Scheme 1. As the reduction of the metal ion occurs only in alkaline medium, naturally the indole NH group is deprotonated, which subsequently donates an electron to the nearby metal ion forming a neutral tryptophyl radical. The formed radical subsequently reverses back to its native structure, converts to the kynurenine form of the peptide, or dimerizes to a ditryptophan form of the peptide. During this transformation a proton is eliminated, which counter balances the hydroxide ion present in the medium and we observe that the pH of the reaction medium decreases from pH 11 to 8.5 after the completion of the reduction.

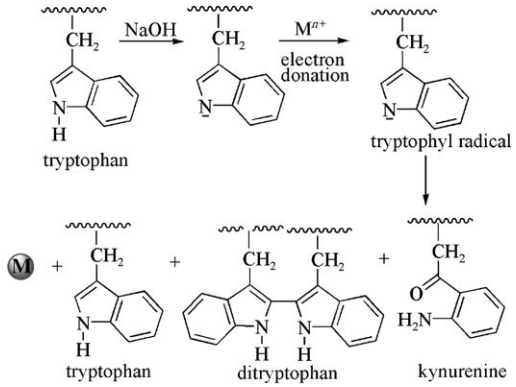

Scheme 1.

Conclusion

Oligopeptides with a tryptophan moiety at the C-terminus were synthesized and used for the synthesis of gold and silver nanoparticles at basic pH. The tryptophan residue present in the peptide was responsible for the reduction of metal ions to the respective metal atoms, which eventually combined to form MNPs. UV-visible and fluorescence spectroscopic studies showed that the tryptophan residue of the peptide was converted to the highly fluorescent forms ditryptophan/kynurenine of the peptide. Based on these studies, a mechanistic pathway for MNP synthesis by using tryptophan-containing peptides has been suggested. According to this mechanism, the tryptophan residue of the peptide donates an electron to the metal ion and is itself converted to a transient tryptophyl radical, which eventually transform to the native tryptophan or ditryptophan/kynurenine form of the peptide.

Experimental Section

Materials: L-Leucine (Leu), α-aminoisobutyric acid (Aib), L-tryptophan (Trp), dicyclohexylcarbodiimide (DCC), and 1-hydroxybenzotriazole (HOBt) were purchased from SRL India and hydrogen tetrachloroaurate(III) trihydrate ($HAuCl_4 \cdot 3H_2O$) was purchased from Sigma-Aldrich. All the aqueous solutions were prepared with triple-distilled water and reagent-grade solvents were used for peptide synthesis.

Peptide Synthesis: Tripeptide-1 (NH_2-Leu-Aib-Trp-OMe) and tripeptide-2 (Boc-Leu-Aib-Trp-OH) were synthesized by conventional solution-phase methods by using a racemization-free fragmentation/condensation strategy. The Boc group was used for N-terminal protection and the C-terminus was protected as a methyl ester. Couplings were mediated by dicyclohexylcarbodiimide/1-hydroxybenzotriazole (DCC/HOBt). All intermediates have been characterized by ^{1}H NMR spectroscopy (300 MHz) and TLC on silica gel and were used without further purification. The final products were purified by column chromatography by using silica gel (100–200 mesh size) as the stationary phase and ethyl acetate/toluene 2:1 as eluent. Purified final compounds have been fully characterized by 300 MHz ^{1}H NMR spectroscopy and ESI-MS.

Boc-Leu-Aib-Trp-OMe: Boc-Leu-Aib-OH[23] (3.16 g, 10 mM) in DMF (20 mL) was cooled in an ice-water bath. H_2N-Trp-OMe, isolated from the corresponding methyl ester hydrochloride (5.08 g, 20 mM) by neutralization with saturated Na_2CO_3 solution and subsequent extraction with ethyl acetate, was added to this solution. Finally, DCC (2.06 g, 10 mM) and HOBt (1.35 g, 10 mM) were added to the above reaction mixture. The reaction mixture was stirred for 3 d in a magnetic stirrer. The resultant product was taken in ethyl acetate (30 mL) and DCU was filtered off. The organic layer was washed with HCl (2 N, 3×20 mL), brine (1×20 mL), sodium carbonate (1 M, 3×20 mL), and brine (2×20 mL). The organic layer was then dried over anhydrous sodium sulfate and evaporated under vacuum. Purification was carried out by silica-gel column chromatography (100–200 mesh) by using ethyl acetate/toluene as the eluent. Yield: 3.87 g (7.5 mM, 75%); ^{1}H NMR (300 MHz, $CDCl_3$, TMS): $\delta = 8.27$ (s, 1H; Trp ring NH), 7.53–7.50 (d, $J = 9.0$ Hz, 1H; Trp ring H), 7.36–7.33 (d, $J = 9.0$ Hz, 1H; Trp ring H), 7.19–7.07 (m, 2H; Trp ring Hs), 7.04–7.03 (d, $J = 3.0$ Hz, 1H; Trp ring Hs), 6.86–6.84 (d, $J = 6.0$ Hz, 1H; Trp NH), 6.49 (s, 1H; Aib NH), 4.89–4.83 (m, 1H; Trp C^α–H), 4.80–4.78 (d, $J = 6.0$ Hz, 1H; Leu NH), 4.01 (br s, 1H; Leu C^α–H), 3.66 (s, 3H; OCH_3), 3.33–3.30 (m, 2H; Trp C^β–Hs), 1.66–1.54 (m, 3H; Leu C^β–H, C^γ–H), 1.50 (s, 6H; Aib C^β–H), 1.43 (s, 9H; Boc H), 0.92–0.90 ppm (d, $J = 6.0$ Hz, 6H; Leu C^δ–H); MS (35 eV): m/z (%): 539 (100) $[M+Na]^+$; elemental analysis calcd. (%) for $C_{27}H_{40}N_4O_6$ (516): C 62.79, H 7.75, N 10.85; found: C 62.05, H 7.56, N 9.95.

Peptide-1 (NH_2-Leu-Aib-Trp-OMe): Formic acid (10 mL, 98%) was added to Boc-Leu-Aib-Trp-OMe (2.58 g, 5 mM) and the subsequent removal of the Boc group was monitored by TLC. After, 8 h, the formic acid was removed under vacuum. The residue was then dissolved in water (20 mL) and washed with diethyl ether (2×20 mL). The pH of the aqueous solution was adjusted to pH 8 with sodium bicarbonate and extracted with ethyl acetate (3×30 mL). The organic extracts were pooled, washed with saturated brine, dried over sodium sulphate, and concentrated to a viscous liquid which gave a positive ninhydrin test. Yield: 1.55 g, 60%; ^{1}H NMR (300 MHz, $CDCl_3$, TMS): $\delta = 8.33$ (s, 1H; Trp ring NH), 7.73 (s, 1H; Aib NH), 7.55–7.52 (d, $J = 9.0$ Hz, 1H; Trp ring H), 7.36–7.33 (d, $J = 9.0$ Hz, 1H; Trp ring H), 7.25–7.02 (m, 3H; Trp ring H), 4.89–4.83 (m, 1H; Trp C^α–H), 4.15–4.08 (m, 1H; Leu C^α–H), 3.67 (s, 3H; OCH_3), 3.38–3.21 (m, 4H; Trp C^β–H, Leu C^β–H), 1.49 (s, 6H; Aib C^β–H), 0.91–0.87 ppm (m, 6H; Leu C^δ–H); MS (35 eV): m/z (%): 439 (100) $[M+Na]^+$; elemental analysis calcd (%) for $C_{22}H_{32}N_4O_4$ (416): C 63.46, H, 7.69, N 13.46; found: C 63.1, H 7.75, N 13.5.

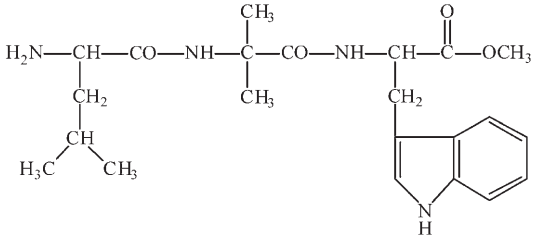

Peptide-2 (Boc-Leu-Aib-Trp-OH): MeOH (25 mL) and NaOH (2 M, 10 mL) were added to Boc-Leu-Aib-Trp-OMe (2.58 g, 5 mM) and the progress of saponification was monitored by TLC. The reaction mixture was stirred with a magnetic stirrer for 10 h and then the methanol was removed under vacuum. The residue was dissolved in water (30 mL) and washed with diethyl ether (2×20 mL). Then the pH of the aqueous layer was adjusted to pH 2 by using HCl (1 M) and it was extracted with ethyl acetate (3×20 mL). The extracts were pooled, dried over anhydrous sodium sulfate, and evaporated under vacuum to yield 2.00 g of a white solid. Yield: 2.00 g (4 mmol, 80%); ^{1}H NMR (300 MHz, $CDCl_3$+5% DMSO, TMS): $\delta = 9.12$ (s, 1H; Trp ring NH), 7.62–7.59 (d, $J = 9.0$ Hz, 1H; Trp ring H), 7.35–7.32 (d, $J = 9.0$ Hz, 1H; Trp ring H), 7.15–7.02 (m, 3H; Trp ring H), 6.88–6.86 (d, $J = 6.0$ Hz, 1H; Trp NH), 5.34–5.32 (d, $J = 6.0$ Hz, 1H; Leu NH), 4.82–4.76 (m, 1H; Trp C^α–H), 4.08 (br s, 1H; Leu C^α–H), 3.42–3.28 (m, 2H; Trp C^β–H), 1.68–1.57 (m, 3H; Leu C^β–H, C^γ–H), 1.49 (s, 6H; Aib C^β–H), 1.42 (s, 9H; Boc H), 0.93–0.90 ppm (m, 6H; Leu C^δ–H); MS (35 eV): m/z (%): 525 (100) $[M+Na]^+$; elemental analy-

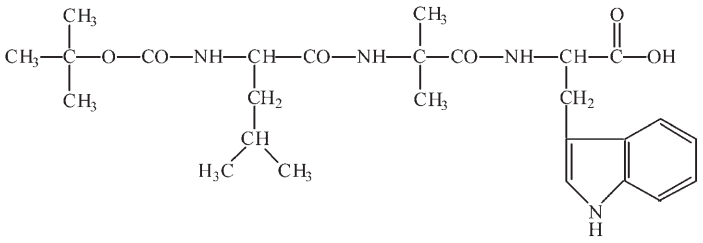

sis calcd (%) for $C_{26}H_{38}N_4O_6$ (502): C 62.15, H 7.57, N 11.15; found: C 60.01, H 7.17, N 11.15.

Gold–peptide nanoconjugates (peptide–GNPs): In a typical preparation, a mixture of peptide-1 (0.25 mL, 40 mM solution in methanol) and triple-distilled water (1.25 mL) was added dropwise to an aqueous solution of $HAuCl_4$ (0.5 mL, 10 mM) with constant stirring. The mixture pH was then adjusted to pH ≈11 with standard NaOH solution. The final reaction mixture was stirred for 3 d at room temperature. A color change was observed from yellow to ruby red, indicating the formation of colloidal GNPs by oxidation of the tryptophan residue of peptide-1.

Similarly, GNPs were also synthesized simply by replacing peptide-1 by -2 whilst keeping the other parameters constant.

Silver–peptide nanoconjugates (peptide–SNPs): An aqueous solution of $AgNO_3$ (0.2 mL, 10 mM) was added to a mixture of peptide-1 (0.25 mL, 40 mM solution in methanol) and triple-distilled water (1.65 mL), and the reaction mixture was kept stirring for 2 min. After this time, the pH of the mixture was adjusted to ≈11 with standard NaOH solution. The reaction was stirred for 3 d at room temperature. In this case, a color change from colorless to yellow was observed, indicating the formation of colloidal silver nanoparticles by oxidation of tryptophan residue of peptide-1.

Similarly, peptide-2 was used for synthesizing SNPs by simply replacing peptide-2 with -1 whilst keeping the other parameters constant.

Characterization: All NMR spectroscopic experiments were carried out in by using Bruker DPX 300 MHz spectrometers at 300 K. Peptide concentrations were in the range 1–10 mM. ESI mass spectra of dilute solutions of peptides in methanol were recorded by using a quadrupole time-of-flight (Qtof) Micro YA263 mass spectrometer. Elemental analyses of the purified peptides were carried out by using a Perkin–Elmer 2400 series II CHN analyzer. UV-visible absorption spectra of the diluted as-prepared peptide–GNP/peptide–SNP colloidal suspensions were recorded by using a Hewlett–Packard 8453 UV-visible spectrophotometer. One drop of the as-prepared peptide-GNP/peptide-SNP suspensions was placed on a carbon-coated copper grid and allowed to air dry. The grid was then observed under a JEOL high-resolution transmission electron microscope (TEM) and imaged at an accelerating voltage of 200 KV. FTIR spectra of the neat peptide-1 and peptide-1–GNP conjugates were recorded from KBr pellets, prepared by mixing the corresponding dried sample with KBr in a 1:100 (wt/wt) ratio by using a Shimadzu FTIR-8400S spectrometer. Thermogravimetric analysis (TGA) of the dry powdered peptide–GNPs conjugates, obtained by centrifugation, was carried out by using a PYRIS Diamond TG/DTA (Perkin–Elmer) instrument. Emission spectra of peptide solution/peptide–GNPs suspension/supernatant containing the oxidized form of the peptide were recorded on a Hitachi F-2500 spectrofluoremeter.

Acknowledgements

S. Si thanks the Council of Scientific and Industrial Research, Govt. of India for providing the fellowship. This research was supported by grants from the Department of Biotechnology, New Delhi. Thanks are also due to the partial support from the Nanoscience and Nanotechnology Initiatives, DST, New Delhi.

[1] C. K. Kim, R. R. Kalluru, J. P. Singh, A. Fortner, J. Griffin, G. K. Darbha, P. C. Ray, *Nanotechnology* **2006**, *17*, 3085–3093.
[2] J. W. Liu, Y. Lu, *J. Fluoresc.* **2004**, *14*, 343–354.
[3] X. Luo, A. Morrin, A. J. Killard, M. R. Smyth, *Electroanalysis* **2006**, *18*, 319–326.
[4] A. Gole, C. Dash, V. Ramakrishnan, S. R. Sainkar, A. B. Mandale, M. Rao, M. Sastry, *Langmuir* **2001**, *17*, 1674–1679.
[5] R. Narayanan, M. A. El-Sayed, *J. Phys. Chem. B* **2005**, *109*, 12663–12676.
[6] J. J. Storhoff, R. Elghanian, R. C. Mucic, C. A. Mirkin, R. L. Letsinger, *J. Am. Chem. Soc.* **1998**, *120*, 1959–1964.
[7] S. Liang, D. T. Pierce, C. Amiot, X. J. Zhao, *Synth. React. Inorg. Met.-Org. Nano-Met. Chem.* **2005**, *35*, 661–668.
[8] S. G. Penn, L. He, M. J. Natan, *Curr. Opin. Chem. Biol.* **2003**, *7*, 609–615.
[9] U. Kreibig, M. Vollmer, *Optical Properties of Metal Clusters*, Springer-Verlag, Berlin, **1995**.
[10] R. R. Bhattacharjee, M. Chakraborty, T. K. Mandal, *J. Phys. Chem. B* **2006**, *110*, 6768–6775.
[11] M. A. Hayat, *Colloidal Gold: Principles, Methods, and Applications*, Academic Press, San Diego, CA, **1991**.
[12] M. Aslam, L. Fu, M. Su, K. Vijayamohanan, V. P. Dravid, *J. Mater. Chem.* **2004**, *14*, 1795–1797.
[13] P. R. Selvakannan, S. Mandal, S. Phadtare, A. Gole, R. Pasricha, S. D. Adyanthaya, M. Sastry, *J. Colloid Interface Sci.* **2004**, *269*, 97–102.
[14] R. C. Prince, *Trends Biochem. Sci.* **1988**, *13*, 286–288.
[15] B. M. Hoffman, J. E. Roberts, C. H. Kang, E. Margoliash, *J. Biol. Chem.* **1981**, *256*, 6556–6564.
[16] M. Sivaraja, D. B. Goodin, M. Smith, B. M. Hoffman, *Science* **1989**, *245*, 738–740.
[17] M. Sahlin, G. Lassmann, S. Potsch, A. Slaby, B.-M. Sjoberg, A. Graslund, *J. Biol. Chem.* **1994**, *269*, 11699–11702.
[18] F. Lendzian, M. Sahlin, F. MacMillan, R. Bittl, R. Fiege, S. Potsch, B.-M. Sjoberg, A. Graslund, W. Lubitz, G. Lassmann, *J. Am. Chem. Soc.* **1996**, *118*, 8111–8120.
[19] C. Essenmacher, S. T. Kim, M. Atamian, G. T. Babcock, A. Sancar, *J. Am. Chem. Soc.* **1993**, *115*, 1602–1603.
[20] P. F. Heelis, T. Okamura, A. Sancar, *Biochemistry* **1990**, *29*, 5694–5698.
[21] F. Himo, L. A. Eriksson, *J. Phys. Chem. B* **1997**, *101*, 9811–9819.
[22] Y. Zhou, W. Chen, H. Itoh, K. Naka, Q. Ni, H. Yamane, Y. Chujo, *Chem. Commun.* **2001**, 2518–2519.
[23] R. R. Bhattacharjee, A. K. Das, D. Haldar, S. Si, A. Banerjee, T. K. Mandal, *J. Nanosci. Nanotechnol.* **2005**, *5*, 1141–1147.
[24] J. M. Slocik, R. R. Naik, M. O. Stone, D. W. Wright, *J. Mater. Chem.* **2005**, *15*, 749–753.
[25] P. R. Selvakannan, A. Swami, D. Srisathiyanarayanan, P. S. Shirude, R. Pasricha, A. B. Mandale, M. Sastry, *Langmuir* **2004**, *20*, 7825–7836.
[26] S. Si, R. R. Bhattacharjee, A. Banerjee, T. K. Mandal, *Chem. Eur. J.* **2006**, *12*, 1256–1265.
[27] J. A. Creighton, D. G. Eadon, *J. Chem. Soc. Faraday Trans.* **1991**, *87*, 3881–3891.
[28] N. F. Mott, E. A. Davis, *Electron Processes in Non-Crystalline Materials*, Clarendon Press, Oxford, UK, **1971**.
[29] M. R. DeFelippis, C. P. Murthy, M. Faraggi, M. H. Klapper, *Biochemistry* **1989**, *28*, 4847–4853.
[30] D. G. Duff, A. Baiker, P. P. Edwards, *Langmuir* **1993**, *9*, 2301–2309.
[31] H. Zhang, C. Andrekopoulos, J. Joseph, K. Chandran, H. Karoui, J. P. Crow, B. Kalyanaraman, *J. Biol. Chem.* **2003**, *278*, 24078–24089.
[32] L. B. Anderson, M. Maderia, A. J. Ouellette, C. Putnam-Evans, L. Higgins, T. Krick, M. J. MacCoss, H. Lim, J. R. Yates, B. A. Barry, *Proc. Natl. Acad. Sci. USA* **2002**, *99*, 14676–14681.
[33] S. Vazquez, J. A. Aquilina, J. F. Jamie, M. M. Sheil, R. J. Truscott, *J. Biol. Chem.* **2002**, *277*, 4867–4873.

[34] D. W. Cleveland, J. D. Rothstein, *Nat. Rev. Neurosci.* **2001**, *2*, 806–819.
[35] J. A. Aquilina, J. A. Carver, R. J. Truscott, *Biochemistry* **2000**, *39*, 16176–16184.
[36] J. A. Aquilina, J. A. Carver, R. J. Truscott, *Biochemistry* **1999**, *38*, 11455–11464.
[37] S. J. Stachel, R. L. Habeeb, D. A. Van Vranken, *J. Am. Chem. Soc.* **1996**, *118*, 1225–1226.
[38] Z. Zhang, A. Berg, H. Levanon, R. W. Fessenden, D. Meisel, *J. Am. Chem. Soc.* **2003**, *125*, 7959–7963.
[39] P. Ionita, A. Caragheorgheopol, B. C. Gilbert, V. Chechik, *J. Am. Chem. Soc.* **2002**, *124*, 9048–9049.
[40] D. Kivelson, *J. Chem. Phys.* **1960**, *33*, 1094–1106.
[41] D. J. Maxwell, J. R. Taylor, S. Nie, *J. Am. Chem. Soc.* **2002**, *124*, 9606–9612.
[42] A. C. Pineda, D. Ronis, *J. Chem. Phys.* **1985**, *83*, 5330–5337.
[43] I. Pockrand, A. Brillante, D. Mobius, *Chem. Phys. Lett.* **1980**, *69*, 499–504.

Received: October 19, 2006
Published online: January 24, 2007

